Strong crystal field effect in $Np^{4+}:ThCl_4$ - optical absorption study

1998 J. Phys.: Condens. Matter 10 11841

(http://iopscience.iop.org/0953-8984/10/50/021)

J. Phys.: Condens. Matter **10** (1998) 11841–11855. Printed in the UK PII: S0953-8984(98)97633-0

Strong crystal field effect in Np^{4+}:$ThCl_4$—optical absorption study

Z Gajek†§ and J C Krupa‡

† Instytut Niskich Temperatur i Badań Strukturalnych, Polska Akademia Nauk, 50-950 Wrocław 2, Skr. Poczt. 1410, Poland

‡ Laboratoire de Radiochimie, Institut de Physique Nucléaire, BP 1, 91406 Orsay Cédex, France

Received 16 September 1998

Abstract. Results of optical absorption measurements in polarized light on tetravalent neptunium diluted in a $ThCl_4$ single crystal are reported. The recorded spectra are complex, pointing to the presence of an Np^{3+} impurity. The electronic transitions assigned to the Np^{4+} ion are interpreted in terms of the usual model, following the actual understanding of the neptunium electronic structure and independent theoretical predictions. R.m.s. deviations of the order of 36 cm^{-1} have been obtained for 42 levels fitted with 11 free parameters. The crystal field effect resulting from the fitting is considerably larger than that observed for the uranium ion in the same host.

1. Introduction

Very few investigations of optical spectra of the Np^{4+} ion in a crystal resulting in detailed electronic structure determination have been published so far [1–13]. First trials were undertaken in 1969 for Np^{4+}:$PbMoO_4$ [1] and Np^{4+}:ThO_2 [2]. These studies, as well as two others of that time [3, 4], were limited to the lowest few multiplets. Contemporary computation skills did not allow progress beyond the Russell–Saunders coupling scheme. The papers set forth, however, some idea about the neptunium electronic structure and evidenced the necessity of a simultaneous diagonalization of all main interactions determining the neptunium $5f^3$ electronic structure in solids. The last requirement could be met ten years later for the $Np(BD4)_4/Zr(BD4)_4$ system [5]. As many as 46 zero phonon transitions were assigned starting from a much larger number of observed lines with the r.m.s. error of 84 cm^{-1}. Another trial has been undertaken for the $ZrSiO_4$ matrix [6]. Of 44 identified firm transitions of the expected polarization characteristic only 31 had a reasonable r.m.s. deviation. More precise fitting was possible for Np^{4+}:$ThSiO_4$ [7–10] where an apparently weaker crystal field effect was observed. The later Np^{4+}:ThO_2 study [7, 9], extending the initial one [2], has pointed to the cubic symmetry and vibronic character of the observed excitations in this system. The limited number of levels assigned did not allow, however, more than qualitative discussion.

An example of extremely complicated neptunium spectra has been reported for the low symmetry system NpF_4 [11], in which transitions corresponding to two non-equivalent metal sites have been observed. It was tractable with the aid of the superposition model constraints and other assumptions, which were questioned later [12, 13]. In particular, the authors did

§ E-mail address: gajek@int.pan.wroc.pl.

0953-8984/98/5011841+15$19.50

not present convincing arguments that the lines they assigned belong to the same metal site or that those coming from different sites are close enough to each other.

Strong JJ mixing and a large number of levels make the Np^{4+} ($5f^3$) spectra especially difficult for interpretation. In addition, the higher order correlation effects, which are not included in the common model, are expected to be important. An essential role of the configuration interaction effects in elimination of evident discrepancies characteristic for the conventional approach has been demonstrated for such ions as Nd^{3+} ($4f^3$) or U^{4+} ($5f^2$) [14, 15].

Extended experimental material analysed in the frame of the conventional approach is necessary to understand the main features of the neptunium electronic structure and eventually the higher order effects. Taking into account the number of available optical spectroscopy studies on Np^{4+} and the problems arising there (see review papers [9] and [16]), it is obvious that we are just at the beginning of the way. The actual discussion still concerns basic points such as the range of nephelauxetic reduction of f electron Coulomb repulsion or the order of magnitude of the ordinary crystal field effect (see a characteristic example of discussion for actinide dioxides [17]).

In the present paper we report optical absorption investigations of the Np^{4+} ion diluted in a $ThCl_4$ matrix. This interesting tetragonal host capable of measurements in polarized light has been used in electronic structure study of such doped ions as protactinium [18] and uranium [19]. The latter has been widely investigated and served here as one of the important reference points. We follow also the electronic structure of Np^{4+} in $ThSiO_4$ and $ZrSiO_4$ matrices mentioned above.

A real problem is the presence of the Np^{3+} impurity in our samples. To separate the Np^{3+} and Np^{4+} spectra we took into account a difference in the electric dipole selection rules characteristic for various polarizations of light and some other indications deduced from selectively excited emission measurements as well as literature data concerning possible locations of Np^{3+} bands [20].

The crystal field effect was discussed with aid of numerical simulations based on a first-principle perturbation model developed for actinide ionic systems [21].

The paper is organized as follows. The next section provides the experimental details followed by the description of the spectra. The parametric analysis is given in section 4 and section 5 closes with discussion and conclusions.

2. Experiment

Thorium tetrachloride was prepared by direct reaction of thorium metal and chlorine at 900 °C. Single crystals were prepared by the Bridgman method. $ThCl_4$ was doped with about 0.1% of Np^{4+}, the doping material being NpO_2. The material was transferred to a crystal growing silica tube in an inert-atmosphere dry box.

X-ray analysis has shown the product to be a single crystal that could be indexed in the tetragonal system $I4_1/amd_1$ [22]. The point group symmetry at the thorium/neptunium site is D_{2d}. Eight chlorine ions around the neptunium ion form two interpenetrating tetrahedra twisted mutually by 90°. At 70 K, $ThCl_4$ undergoes a displacive phase transition to an incommensurate phase [19, 23]. This may cause a broadening of some observed optical absorption lines in the low temperature spectrum.

The absorption spectra were recorded at 4.2, 77 K and room temperature in the visible and infrared region on a 'CARY model 17' and a one metre 'HR 1000 Jobin Yvon' spectrometer equipped with a 1200 and 600 lines mm^{-1} grating photomultiplier and PbS detector respectively.

Emission spectra were induced by nitrogen laser radiation or excited selectively with an N_2 laser pumped dye laser.

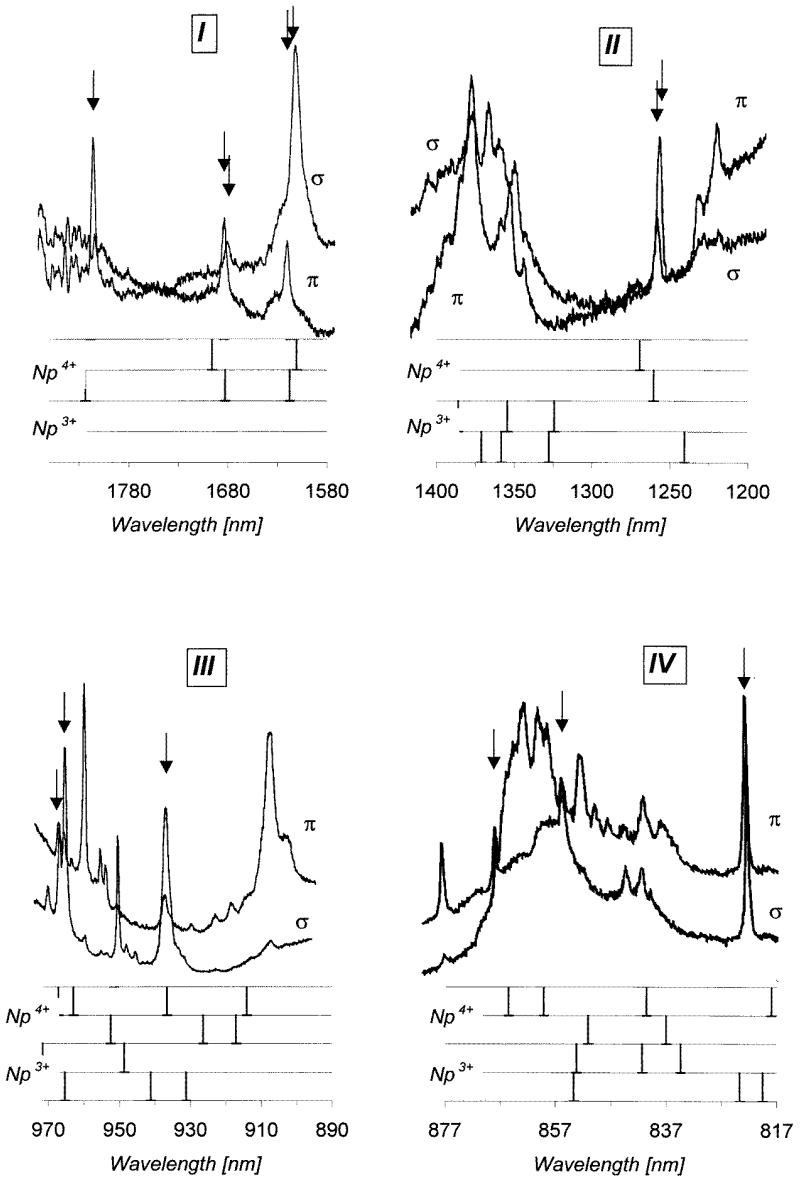

(a)

Figure 1. Absorption spectra observed for neptunium ion in $ThCl_4$ matrix and below—positions of calculated Np^{4+} ($\sigma\pi$, σ) and estimated Np^{3+} (σ, π) transitions (see the main text for details) in infrared (a) and visible (b).

3. Description of the spectra

The spectra recorded in σ and π polarization of light are shown in figure 1. The observed lines are listed in table 1.

The Kramers degenerate states of Np^{4+} ($5f^3$) in D_{2d} symmetry are classified by Γ_6 and Γ_7 double group representation. The $\Gamma_6 \rightarrow \Gamma_6$ and $\Gamma_7 \rightarrow \Gamma_7$ transitions are allowed

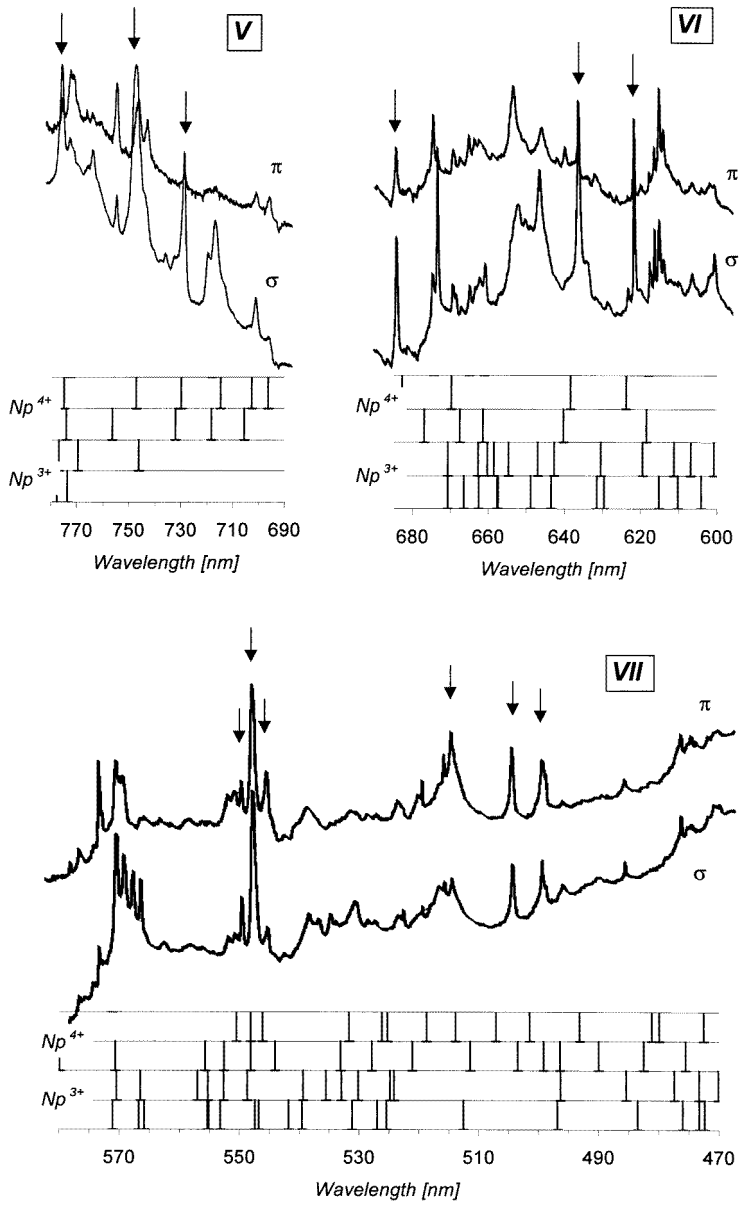

(b)

Figure 1. (Continued)

for σ polarization of light only. The transitions $\Gamma_6 \rightarrow \Gamma_7$ and $\Gamma_7 \rightarrow \Gamma_6$ should be seen simultaneously in σ and π polarized spectra.

To be more specific in what follows we have assumed Γ_6 to be the ground state. It has been found to be the ground state for Np^{4+}:$ThSiO_4$ and Np^{4+}:$ZrSiO_4$ systems, which have the same both space and point symmetries. Preliminary calculations with CF parameters taken from U^{4+}:$ThCl_4$ as well as these determined from *ab initio* calculations (see next

Table 1. Absorption spectrum of Np^{4+} and Np^{3+} in $ThCl_4$. Transitions typed in italic have not been included in the parametric analysis of Np^{4+} electronic structure. The levels in the visible region from which fluorescence has been observed are indicated.

Wavelength [nm]	Transition energy [cm^{-1}]	Intensity[a,b] σ	Intensity[a,b] π	Wavelength [nm]	Transition energy [cm^{-1}]	Intensity[a,b] σ	Intensity[a,b] π	Fluorescence[b]
Zone I				717.9	13 926	m	—	
1818.4	5498	s	—	702.5	14 231	w	w	
1687.5	5924	m, sh	m	697.3	14 337	vw	w	
1684.2	5936	m	—	Zone VI				
1622.7	6161	m, sh	m	683.4	14 629	s	m	
1616.0	6186	s	—	*679.3*	*14 717*	*vw*	—	
Zone II				674.3	14 826	m	—	
1377.1	*7260*	*m*	*s*	*673.9*	*14 835*	—	*s*	
1369.4	*7300*	*m*	—	*673.0*	*14 855*	*s*	*m*	*s*
1361.2	*7344*	*w*	*vw*	*669.2*	*14 939*	*m*	—	
1354.1	*7383*	—	*m*	669.0	14 944	—	m	
1352.9	*7390*	*m*	—	*666.9*	*14 991*	*?*	*w*	
1347.1	*7421*	—	*w*	664.9	15 036	w	m	
1267.0	7891	m, sh	m	*662.3*	*15 095*	*w*	—	
1265.1	7902	s	—	*662.0*	*15 102*	—	*m*	
1240.0	*8062*	—	*w*	661.0	15 124	m	—	
1229.0	*8134*	—	*m*	*660.9*	*15 127*	—	*m*	
Zone III				*652.6*	*15 319*	*w*	—	
1038.5	*9627*	*w*	—	*650.8*	*15 361*	*vw*	—	
1022.4	*9779*	*vw*	—	*647.2*	*15 447*	*m*	—	
1003.8	*9959*	*w*	*w*	*646.7*	*15 459*	*w*	*sh?*	
1002.9	*9968*	*w*	—	637.3	15 687	s	m	
1001.3	*9984*	*w*	*w*	635.1	15 741	w		
999.2	*10 005*	*w*	*w*	*629.7*	*15 876*	*vw*		
989.2	*10 106*	*vw*	—	623.1	16 044	s	m	
986.6	*10 133*	*w*	—	*619.4*	*16 140*	*w*	*vw*	
985.4	*10 145*	*vw*	—	*619.0*	*16 151*	*w?*	—	
971.6	*10 289*	*w*	—	617.7	16 184	m	w	
968.3	10 325	m	m	*616.8*	*16 208*	*m*	*m*	
966.7	10 342	s	m	*615.8*	*16 235*	*vw*	*w*	
960.9	*10 404*	*vw*	*s*	Zone VII				
956.1	*10 456*	—	*m*	*573.7*	*17 427*	*w*	*s*	
954.5	*10 474*	—	*m*	571.0	17 509	s	s	
951.4	10 508	s	vw	*569.7*	*17 547*	*m*	*m*	
948.9	*10 536*	*vw*	—	*568.3*	*17 592*	*m*	*vw?*	
946.2	*10 566*	*vw*	—	*567.0*	*17 631*	*m*	*vw?*	*m*
937.7	10 661	s	m	*552.5*	*18 093*	*w*	*w*	*s*
906.5	*11 029*	*vw*	*s*	*551.3*	*18 134*	*w*	*w*	*s*

section) justify this assumption. We have checked also several assignation possibilities with Γ_7 ground state, but no satisfactory solutions have been found; moreover, the iteration procedure always turned back to the Γ_6 ground state.

The π only transitions seen in the spectra, figure 1, point to the presence of an Np^{3+} ($5f^4$) impurity. This complicates further analysis. The selection rules for f^4 configurations permit either pure σ or pure π transitions. Thus any transition observed simultaneously in σ and π recording has to belong in principle to the Np^{4+} ion. Since the spectra of Np^{4+} and Np^{3+} overlap, an accidental coincidence of the σ line coming from the Np^{4+} ion with

Table 1. (Continued)

Wavelength [nm]	Transition energy [cm^{-1}]	Intensity[a,b] σ	Intensity[a,b] π	Wavelength [nm]	Transition energy [cm^{-1}]	Intensity[a,b] σ	Intensity[a,b] π	Fluorescence[b]
Zone IV				550.4	18 165	m	w	w
876.9	*11 401*	*vw*	*s*	548.5	18 226	s	s	vw?
867.4	11 526	m	m	546.1	18 306	w	m	w
865.2	*11 555*	*s*	—	*539.1*	*18 545*	*m*	*m*	*m*
864.1	*11 570*	*s*	—	*537.4*	*18 602*	*w*	—	
862.4	*11 592*	*vs*	—	*536.0*	*18 653*	*w*	—	
859.6	*11 630*	*vs*	—	531.6	18 805	m	w	
857.9	*11 653*	*s*	—	*524.4*	*19 065*	*w*	*w*	
855.4	11 687	m	m	523.5	19 096	w	w, sh	m
844.1	11 843	w	w	520.4	19 210	w	m	s
840.6	11 893	m	m	*517.9*	*19 302*	*s*	—	*w*
839.5	*11 909*	*vw*	—	*516.7*	*19 348*	*s*	*s*	
821.8	12 165	s	s	515.7	19 387	s	s	w
Zone V				505.7	19 768	s	s	s
775.3	12 895	s	m	500.8	19 964	s	s	s
763.9	*13 087*	*w*	*w*	*500.1*	*19 989*	*sh*	*sh*	
755.0	*13 241*	*w*	*m*	*497.2*	*20 106*	*w*	*vw*	
748.0	13 365	s	w	*487.1*	*20 525*	*w*	*w*	
747.5	*13 374*	*m, sh*	*m*	*478.0*	*20 916*	*w*	*w*	
729.6	13 702	s	w	*476.3*	*20 989*	*vw*	*w*	
720.1	*13 883*	*w*	—					

[a] σ and π denote polarization of light.
[b] The intensity is specified as follows: vs—very strong, s—strong, m—medium, w—weak, vw—very weak, sh—shoulder.

the π line from Np^{3+} cannot be excluded. To discern areas where the Np^{3+} bands are expected we follow the investigations for Np^{3+} in $LaCl_3$ [20].

The whole Np^{4+} absorption spectrum may be partitioned into seven regions characteristic for this ion as shown in table 2.

Table 2. Absorption regions characteristic of the Np^{4+} ion.

Zone	Wavelength [nm]	Energy [cm^{-1}]
I	1800–1610	5375–6209
II	1300–1200	7690–8331
III	980–910	10 201–10 986
IV	877–817	11 399–12 237
V	780–690	12 817–14 489
VI	690–600	14 489–16 662
VII	580–490	17 237–20 402

The first four zones contain well separated groups of levels of similar LSJ components. The zones V–VII have been distinguished to focus one's attention on each of the three parts of the visible region, where wide and complicated bands are observed.

The two first IR zones, I and II, are of special importance because they are free of Np^{3+} transitions. The first group corresponds to the $^4I_{11/2}$ term for which three Γ_6 and three Γ_7 levels are expected. According to the electric dipole selection rules six σ lines can be

expected here, three of which should be accompanied by π components. Actually, we see three σ and two π structures only. Since π lines are shifted with respect to their σ partners, the latter are supposed to be complex, consisting of two σ lines each: one corresponding exactly to the position of the π partner and the second to a pure σ transition. Similar arguments hold for the lines observed in region II where the D_{2d} crystal field effect leads to the splitting of the $^4F_{3/2}$ term into one Γ_6 and one Γ_7 state. Following our assumption concerning the ground state (Γ_6) all lines observed in both σ and π recordings have to have Γ_7 symmetry. The arrows in figure 1 indicate the most reliable electronic transitions attributed to the Np^{4+} ion. Note that there is only one missing Γ_7 state in zone I.

Table 3. Results of *ab initio* calculations of the CFPs for U^{4+}, Np^{4+} and Np^{3+} ions in a $ThCl_4$ matrix[a] (in cm^{-1}). The contributions of the two co-ordination tetrahedra are specified for each metal ion.

	Contribution	B_{20}	B_{40}	B_{44}	B_{60}	B_{64}	$N_v(4\pi)^{-1/2}$[b]
U^{4+}	Tetrahedral I	−3036	997	2161	−177	−466	1740
	Tetrahedral II	2354	−310	142	−866	439	1100
	Remaining [c]	−595	1016	2588	−119	−182	1296
	Total	−1277	1703	4891	−1162	−209	2465
Np^{4+}	Tetrahedral I	−2585	860	1865	−159	−417	1490
	Tetrahedral II	2002	−262	120	−735	373	935
	Remaining[c]	−547	859	2187	−93	−142	1099
	Total	−1131	1457	4173	−987	−187	2107
Np^{3+}	Tetrahedral I	−3261	661	1432	−81	−212	1624
	Tetrahedral II	2651	−248	114	−557	282	1205
	Remaining[c]	−636	1289	3283	−196	−299	1636
	Total	−1246	1702	4829	−833	−229	2424
	$B_{kq}(Np^{3+})/B_{kq}(Np^{4+})$	1.102	1.168	1.157	0.844	1.225	
	$B_{kq}(Np^{4+})/B_{kq}(U^{4+})$	0.885	0.855	0.853	0.849	0.893	

[a] Crystallographic data have been taken from [22].
[b] CF strength parameter defined as $N_v(4\pi)^{-1/2} = (\Sigma(B_{kq})^2/(2k+1))^{1/2}$ [26].
[c] Point charge contribution of the rest of the crystal and contribution of all the electric dipole multipoles induced in the crystal.

Group III corresponds to the $^4I_{13/2}$ multiplet, which splits into four Γ_6 and three Γ_7. Due to the JJ mixing the actual number of levels may be different. Anyway, all three Γ_7 lines can easily be found in the spectrum. A fourth strong line seen in the σ recording at 951.4 nm may be safely attributed to Γ_6.

Some pure π structures are observed outside the bands reported for Np^{3+}:$LaCl_3$ [20]. This indicates that we cannot treat this reference spectrum too strictly. The actual Np^{3+} band is probably shifted by several hundred cm^{-1} towards higher energies. A similar shift with respect to the Np^{3+}:$LaCl_3$ spectrum takes place in zone V.

To clarify this point we have made several simulations of Np^{3+} spectra using the conventional model described in the next section. The results of one of them shown in figure 1 have been obtained with the free-ion parameters for Np^{3+}:$LaCl_3$ taken from [20] and the crystal field parameters (CFPs) known for U^{4+}:$ThCl_4$ [19]. In other simulations we use final CFPs obtained in the present study for Np^{4+}. The distribution of the levels in these two approaches is different. We did not try to do any fits for Np^{3+} at the present

stage. Our calculations evidence however the possibility of location of Np^{3+}:$ThCl_4$ levels in foreseen areas.

Sharp intense lines observed simultaneously in σ and π recordings, i.e. apparent $\Gamma_6 \rightarrow \Gamma_7$ transitions, distinguished by arrows in figure 1, have been accepted in the zones IV–VII in the initial steps. Special attention has been paid to the regions IV and V, where the Np^{3+} transitions are not so dense as in the zones VI and VII. In particular two less intense $\sigma\pi$ structures at 867.4 nm and 855.2 nm in zone IV have been included. Strong σ structures seen in this region might be somewhat of a problem, which would be more serious if the final model did not comprise them. Unfortunately, being ahead of the final results, this was just the case. None of the considered σ lines could be attributed to the Np^{4+} model transitions discussed in the next section. As seen from figure 1 however, three of them can be associated with the Np^{3+} impurity after some energy shift in the model level distribution. The high intensity of the controversial lines was not very surprising if compared with the intensities of pure π lines in the same area undoubtedly belonging to the impurity.

The transitions observed in the wavelength range 740–670 nm, zones V and VI happen to fall in the energy gap characteristic for the Np^{3+} ion. Thus, they may be treated as a test of the model electronic structure derived for the Np^{4+} ion. As seen from figure 1, the result is satisfactory.

The structure of the absorption lines is extremely dense in zones VI and VII. To verify various level assignments we carried out the selective laser excitation measurements. The fluorescence has been observed from the lines indicated in table 1. Our final model of the Np^{4+} level structure and assignment shown below was not inconsistent with these measurements.

Hitherto known spectroscopic studies on Np^{4+} indicate that there is a dense band of levels of mainly $^4I_{15/2}$ origin of not very large intensity around and above 673 nm. Actually we see such lines uniformly distributed up to 729 nm at 674.3 nm, 683.4 nm, 702.5 nm, 717.9 nm, to list the more visible ones. In the case of Np^{3+}:$LaCl_3$, an edge of a 2000 cm^{-1} energy gap from 14 887 cm^{-1} corresponding to the 671.5 nm wavelength has been observed. The mentioned simulation of the Np^{3+} electronic structure (see figure 1) results in a 1500 cm^{-1} energy gap from 14 910 cm^{-1}. Such a gap favours a strong fluorescence from Np^{3+} rather than from Np^{4+} since the dense electronic levels in the latter case make non-radiative relaxation processes more probable. The variety of vibronic excitations observed for the $ThCl_4$ host [23] justifies this supposition.

4. Model calculations

Our electronic structure calculations were based on the conventional phenomenological Hamiltonian for a single-configuration system. A detailed description of such a Hamiltonian can be found elsewhere (see [9] and references therein). We recall here only brief definitions of the parameters we use.

The main, well known free ion interactions are represented by Coulomb integrals F^k, $k = 2, 4, 6$, and spin–orbit coupling constant ζ. To insure that the free ion structure is adequately represented we take into account the higher order corrections due to the configuration interaction (CI) and relativistic effects. The two- and three-electron corrections originating from the Coulomb repulsion are expressed in terms of α, β, γ and T^k, $k = 2, 3, 4, 6, 7, 8$, parameters. The relativistic corrections were introduced via P^k, $k = 2, 4, 6$, and M^k, $k = 0, 2, 4$, parameters. Following several preceding papers these fine parameters

Table 4. Calculated and experimental energy levels and main eigenvector components in the $|SLJJ_z\rangle$ basis for the Np^{4+}:$ThCl_4$ system.

Γ	E_{calc}	E_{obs}	ΔE	Eigenvector		
6	0	0	0	−0.89 |3/2, 6, 9/2, 1/2⟩	0.35 |1/2, 5(2), 9/2, 1/2⟩	
7	289	—		−0.76 |3/2, 6, 9/2, 3/2⟩	−0.48 |3/2, 6, 9/2, −5/2⟩	0.31 |1/2, 5(2), 9/2, 3/2⟩
6	441	—		0.88 |3/2, 6, 9/2, −7/2⟩	−0.37 |1/2, 5(2), 9/2, −7/2⟩	
6	682	—		0.86 |3/2, 6, 9/2, 9/2⟩	−0.37 |1/2, 5(2), 9/2, 9/2⟩	
7	1121	—		0.75 |3/2, 6, 9/2, −5/2⟩	−0.46 |3/2, 6, 9/2, 3/2⟩	−0.35 |1/2, 5(2), 9/2, −5/2⟩
7	5324	—		−0.77 |3/2, 6, 11/2, 3/2⟩	−0.46 |3/2, 6, 11/2, −5/2⟩	
6	5482	5498	−16	0.91 |3/2, 6, 11/2, 1/2⟩	0.31 |3/2, 6, 11/2, −7/2⟩	
7	5895	5924	−29	−0.91 |3/2, 6, 11/2, 11/2⟩	0.20 |1/2, 5(2), 11/2, 11/2⟩	
6	5940	5936	4	0.95 |3/2, 6, 11/2, 9/2⟩	−0.21 |1/2, 5(2), 11/2, 9/2⟩	
6	6181	6182	−2	−0.90 |3/2, 6, 11/2, −7/2⟩	0.30 |3/2, 6, 11/2, 1/2⟩	
7	6205	6160	45	0.83 |3/2, 6, 11/2, −5/2⟩	−0.47 |3/2, 6, 11/2, 3/2⟩	
7	7878	7893	−15	−0.70 |3/2, 3, 3/2, 3/2⟩	−0.43 |1/2, 2(1), 3/2, 3/2⟩	
6	7929	7902	27	−0.75 |3/2, 3, 3/2, 1/2⟩	−0.47 |1/2, 2(1), 3/2, 1/2⟩	
7	9721	—		0.69 |3/2, 6, 13/2, 3/2⟩	0.56 |3/2, 6, 13/2, −5/2⟩	
6	9764	—		0.86 |3/2, 6, 13/2, 1/2⟩	0.28 |3/2, 6, 13/2, −7/2⟩	
7	10 339	10 325	14	−0.92 |3/2, 6, 13/2, 11/2⟩	−0.24 |1/2, 7, 13/2, 11/2⟩	
7	10 385	10 342	43	0.88 |3/2, 6, 13/2, −13/2⟩	−0.27 |3/2, 3, 5/2, −5/2⟩	
6	10 501	10 508	−7	0.77 |3/2, 6, 13/2, 9/2⟩	−0.31 |3/2, 6, 13/2, −7/2⟩	
7	10 669	10 661	8	0.67 |3/2, 6, 13/2, −5/2⟩	−0.56 |3/2, 6, 13/2, 3/2⟩	
6	10 793	—		−0.81 |3/2, 6, 13/2, −7/2⟩	0.32 |3/2, 6, 13/2, 1/2⟩	
6	10 905	—		−0.50 |3/2, 3, 5/2, 1/2⟩	0.34 |3/2, 4, 5/2, 1/2⟩	0.34 |3/2, 6, 13/2, 9/2⟩
7	10 941	—		−0.39 |3/2, 3, 5/2, 3/2⟩	0.32 |1/2, 5(2), 9/2, −5/2⟩	
6	11 365	—		0.34 |1/2, 5(2), 9/2, −7/2⟩	−0.31 |1/2, 5(2), 9/2, 9/2⟩	
7	11 556	11 526	30	0.42 |3/2, 3, 5/2, −5/2⟩	−0.33 |1/2, 5(2), 9/2, 3/2⟩	
7	11 641	11 687	−46	−0.54 |3/2, 3, 5/2, 3/2⟩	0.39 |3/2, 4, 5/2, 3/2⟩	
6	11 751	—		−0.42 |3/2, 3, 5/2, 1/2⟩	0.34 |3/2, 4, 5/2, 1/2⟩	−0.32 |1/2, 5(2), 9/2, −7/2⟩
7	11 897	11 892	5	−0.51 |3/2, 3, 5/2, −5/2⟩	−0.30 |1/2, 5(2), 9/2, 3/2⟩	
6	11 953	—		−0.52 |1/2, 5(2), 9/2, 1/2⟩	−0.40 |1/2, 4(1), 9/2, 1/2⟩	0.32 |3/2, 3, 9/2, 1/2⟩
7	12 226	12 167	59	0.59 |3/2, 4, 5/2, −5/2⟩	−0.56 |3/2, 4, 5/2, 3/2⟩	−0.30 |3/2, 3, 5/2, 3/2⟩
7	12 903	12 895	8	0.54 |3/2, 0, 3/2, 3/2⟩	0.34 |3/2, 3, 5/2, −5/2⟩	0.33 |3/2, 3, 3/2, 3/2⟩

Table 4. (Continued)

Γ	E_{calc}	E_{obs}	ΔE	Eigenvector		
6	12 917	12 943	−26	−0.61 |3/2, 0, 3/2, 1/2⟩	−0.39 |3/2, 6, 15/2, 1/2⟩	−0.34 |1/2, 1, 3/2, 1/2⟩
6	13 221	13 241	−16	−0.57 |3/2, 3, 7/2, −7/2⟩	0.36 |3/2, 6, 15/2, 1/2⟩	0.34 |1/2, 4(1), 7/2, −7/2⟩
7	13 381	13 365	16	−0.39 |3/2, 3, 5/2, 3/2⟩	0.36 |3/2, 0, 3/2, 3/2⟩	−0.35 |3/2, 3, 7/2, −5/2⟩
6	13 659	—		0.58 |3/2, 4, 5/2, 1/2⟩	0.48 |3/2, 3, 5/2, 1/2⟩	0.31 |3/2, 6, 15/2, 1/2⟩
7	13 701	13 702	−1	−0.55 |3/2, 6, 15/2, 3/2⟩	−0.35 |3/2, 6, 15/2, −5/2⟩	
6	13 921	13 926	−5	0.56 |3/2, 6, 15/2, 1/2⟩	−0.35 |3/2, 0, 3/2, 1/2⟩	0.34 |3/2, 3, 7/2, −7/2⟩
7	13 986	—		0.46 |3/2, 3, 7/2, −5/2⟩	−0.38 |3/2, 4, 5/2, 3/2⟩	−0.32 |1/2, 4(1), 7/2, −5/2⟩
6	14 174	—		0.73 |3/2, 3, 7/2, 1/2⟩	−0.39 |1/2, 4(1), 7/2, 1/2⟩	
7	14 222	14 231	−9	0.83 |3/2, 6, 15/2, −13/2⟩	0.35 |1/2, 7, 15/2, −13/2⟩	
7	14 359	14 337	22	0.56 |3/2, 3, 7/2, 3/2⟩	−0.36 |1/2, 4(1), 7/2, 3/2⟩	0.34 |3/2, 6, 15/2, 3/2⟩
7	14 643	14 629	14	−0.80 |3/2, 6, 15/2, 11/2⟩	−0.37 |1/2, 7, 15/2, 11/2⟩	
6	14 776	14 826	−50	−0.59 |3/2, 6, 15/2, −15/2⟩	0.54 |3/2, 6, 15/2, −7/2⟩	
7	14 928	14 944	−16	0.68 |3/2, 6, 15/2, −5/2⟩	0.36 |1/2, 7, 15/2, −5/2⟩	−0.36 |3/2, 6, 15/2, 3/2⟩
6	14 981	15 036	−55	0.82 |3/2, 6, 15/2, 9/2⟩	0.39 |1/2, 7, 15/2, 9/2⟩	
6	15 115	15 124	−9	−0.54 |3/2, 6, 15/2, −15/2⟩	−0.46 |3/2, 6, 15/2, −7/2⟩	−0.32 |3/2, 4, 7/2, −7/2⟩
6	15 620	—		−0.73 |3/2, 4, 7/2, 1/2⟩	0.29 |3/2, 6, 15/2, −7/2⟩	
7	15 661	15 687	−26	0.76 |3/2, 4, 7/2, 3/2⟩	−0.37 |3/2, 3, 7/2, 3/2⟩	
7	16 030	16 044	−14	−0.78 |3/2, 4, 7/2, −5/2⟩	0.40 |3/2, 3, 7/2, −5/2⟩	
6	16 166	16 183	−17	−0.72 |3/2, 4, 7/2, −7/2⟩	0.42 |3/2, 3, 7/2, −7/2⟩	
7	17 179	—		0.52 |3/2, 3, 9/2, 3/2⟩	0.40 |3/2, 3, 9/2, −5/2⟩	
6	17 244	—		0.61 |3/2, 3, 9/2, 1/2⟩	0.32 |1/2, 5(2), 9/2, 1/2⟩	−0.32 |3/2, 4, 9/2, 1/2⟩
6	17 524	17 509	15	−0.66 |3/2, 3, 9/2, 9/2⟩	−0.43 |1/2, 5(2), 9/2, 9/2⟩	
6	17 991	—		−0.54 |3/2, 3, 9/2, −7/2⟩	−0.31 |1/2, 5(2), 9/2, −7/2⟩	−0.31 |1/2, 5(2), 11/2, 9/2⟩
6	18 094	—		−0.49 |1/2, 5(2), 11/2, 9/2⟩	0.40 |3/2, 4, 11/2, 9/2⟩	
7	18 161	18 164	−3	0.55 |3/2, 3, 9/2, −5/2⟩	−0.44 |3/2, 3, 9/2, 3/2⟩	0.36 |1/2, 5(2), 9/2, −5/2⟩
7	18 240	18 226	14	0.42 |1/2, 5(2), 11/2, 3/2⟩	−0.30 |3/2, 4, 11/2, 3/2⟩	
6	18 243	—		−0.51 |1/2, 7, 13/2, 1/2⟩	−0.30 |1/2, 5(2), 11/2, 1/2⟩	
7	18 314	18 306	8	−0.66 |1/2, 7, 13/2, 3/2⟩	−0.48 |1/2, 7, 13/2, −5/2⟩	
6	18 380	—		−0.38 |1/2, 7, 13/2, 1/2⟩	−0.33 |1/2, 7, 13/2, −7/2⟩	−0.31 |1/2, 5(2), 11/2, −7/2⟩
6	18 759	—		0.48 |1/2, 7, 13/2, 1/2⟩	−0.48 |1/2, 5(2), 11/2, −7/2⟩	0.37 |3/2, 4, 11/2, −7/2⟩

Table 4. (Continued)

Γ	E_{calc}	E_{obs}	ΔE	Eigenvector		
7	18 810	18 805	5	0.46 $\|1/2, 5(2), 11/2, 11/2\rangle$	0.38 $\|1/2, 5(2), 11/2, -5/2\rangle$	−0.30 $\|3/2, 4, 11/2, 11/2\rangle$
6	18 947	—		−0.33 $\|1/2, 5(2), 11/2, 1/2\rangle$	0.32 $\|1/2, 7, 13/2, -7/2\rangle$	−0.32 $\|1/2, 5(2), 11/2, -7/2\rangle$
7	19 002	—		−0.48 $\|1/2, 5(2), 11/2, -5/2\rangle$	0.36 $\|3/2, 4, 11/2, -5/2\rangle$	0.34 $\|1/2, 5(2), 11/2, 11/2\rangle$
7	19 043	19 096	−53	−0.44 $\|1/2, 7, 13/2, 3/2\rangle$	0.40 $\|1/2, 7, 13/2, -5/2\rangle$	
6	19 198	—		0.45 $\|1/2, 7, 13/2, 9/2\rangle$	−0.42 $\|1/2, 7, 13/2, -7/2\rangle$	−0.33 $\|1/2, 5(2), 11/2, 1/2\rangle$
7	19 282	19 210	72	0.43 $\|1/2, 7, 13/2, -13/2\rangle$	−0.43 $\|1/2, 5(2), 11/2, 3/2\rangle$	
7	19 470	19 387	83	−0.55 $\|1/2, 7, 13/2, -13/2\rangle$	−0.36 $\|1/2, 7, 13/2, -5/2\rangle$	
6	19 559	—		0.55 $\|3/2, 2, 1/2, 1/2\rangle$	0.46 $\|1/2, 1, 1/2, 1/2\rangle$	−0.30 $\|3/2, 2, 5/2, 1/2\rangle$
7	19 722	19 768	−46	0.62 $\|1/2, 7, 13/2, 11/2\rangle$	−0.28 $\|3/2, 4, 9/2, -5/2\rangle$	
6	19 862	—		0.49 $\|1/2, 7, 13/2, 9/2\rangle$	−0.37 $\|3/2, 4, 9/2, -7/2\rangle$	
7	19 936	19 964	−28	0.59 $\|3/2, 4, 9/2, -5/2\rangle$	−0.33 $\|3/2, 2, 5/2, -5/2\rangle$	0.32 $\|1/2, 7, 13/2, 11/2\rangle$
6	20 040	—		−0.49 $\|3/2, 4, 9/2, 9/2\rangle$	0.39 $\|3/2, 2, 5/2, 1/2\rangle$	0.31 $\|1/2, 7, 13/2, 9/2\rangle$

Table 5. Electronic structure parameters of uranium and neptunium ions in $ZrSiO_4$, $ThSiO_4$ and $ThCl_4$.

	$ZrSiO_4$ [6]		$ThSiO_4$ [10]		$ThCl_4$	
Parameter	U^{4+}	Np^{4+}	U^{4+}	Np^{4+}	U^{4+} [19]	Np^{4+} (this paper)
E average			12 440 (895)	28 402 (957)		23 481 (53)
F^2	44 258	47 949	42 984 (773)	46 779 (606)	42 752 (162)	44 815 (246)
F^4	40 293	41 455	40 848 (1980)	39 170 (1196)	39 925 (502)	40 321 (368)
F^6	31 287	26 528	23 734 (2220)	28 616 (1766)	24 519 (479)	25 877 (328)
ζ	1740	2088	1841 (9.6)	2138 (7.5)	1808 (8)	2051 (4)
α	23	39	31.3 (1.9)	27 (1.3)	30.4 (2)	35.9 (1.2)
β		−610	−664.8 (132)	−916.8 (49.2)	−492 (84)	−900
γ		1200	1329 (713)	1345 (464)	1200	1350
T^2		278		200		200
T^3		44		50		50
T^4		64		50		50
T^6		−361		−360		−360
T^7		434		425		425
T^8		353		340		340
M^0		0.88	0.77	0.88		0.88
M^2		0.49	0.43	0.49		0.45
M^3		0.34	0.30	0.34		0.33
P^2		500	−186 (225)	103 (192)		300
P^4		500	−93	52		300
P^6		500	−19	10		300
B_{20}	−2000	−2537	−1013 (121)	−83 (85)	−1054 (117)	−2248 (95)
B_{40}	2000	2304	1098 (256)	1333 (140)	1146	2900 (149)
B_{44}	5125	5281	2639 (241)	3568 (64)	2767 (147)	3903 (109)
B_{60}	−5792	−5065	−3053 (542)	−2152 (138)	−2315 (404)	−3116 (146)
B_{64}	−427	−642	257 (309)	829 (109)	312 (227)	−1719 (138)
R.m.s. error	112	34	71	32	46	36
No of levels	30	31	25	47	25	42
No of param.	11	12	14	14	11	11
$N_v(4\pi)^{-1/2}$[a]	3113	3180	1617	1868	1580	2556

[a] See footnote [b] in table 3.

were fixed at the values close to the *ab initio* values, except α, β and γ, for which the values taken from Np^{4+}:$ThSiO_4$ [10] were accepted.

The non-spherical part of our effective single-configuration Hamiltonian has the form of a sum of one-electron operators determined by crystal field parameters (CFPs) B_{kq}—the coefficients of the CF potential expansion in terms of the normalized spherical harmonic operators. In the case of D_{2d} point symmetry there are five independent CFPs: B_{20}, B_{40}, B_{44}, B_{60} and B_{64}.

To have a preliminary idea about the crystal field effect in the system under study we calculated the CFPs using a first principle perturbative model developed for an ionic f-electron system [21]. The Dirac–Slater self-consistent procedure was applied to obtain the zero order, 'free ion' wave functions of neptunium and chlorine ions. The ions were placed in spherical potential wells determined by the actual Madelung energies. Using the projection and contraction technique the complex metal–ligand interactions were simplified to an effective one-electron potential having the form of a functional of the zero order wave functions. The CFPs were given then by direct integration.

The essential CF contributions revealing the complex nature of the metal–ligand interaction were taken into account explicitly. The renormalization correction due to non-

orthogonality of the zero order wave functions was confirmed to be the most important one. The induced electric multipole contributions determined from the crystal electrostatic equilibrium condition were included in the model also. Due to uncertainty in the ionic polarizabilities of the higher orders we confined the calculations to the induced dipoles. The shielding effect was introduced via shielding coefficients [24]. It is known for 5f systems to reduce considerably the second order CFPs.

The results of calculations for the Np^{4+}, Np^{3+} and U^{4+} ions are given in table 3. The contribution of each of two co-ordination tetrahedra excluding influence of the polarization effects was specified to turn one's attention to their competition in the case of B_{20}, B_{40}, B_{64} parameters. Moderate values of these parameters, especially B_{20} and B_{64}, strongly depend, on the other hand, on details of the crystal structure. Even a slight distortion of the metal co-ordination sphere due to, for instance, a different ionic radius of the doping ions, can lead to a drastic repercussion in CFPs. This means an additional uncertainty in determination of these parameters, which should be borne in mind in further discussion of the CF effect.

Comparing our results obtained for various ions, it is interesting to note that the total values of the corresponding parameters differ less than their components. The total B_{kq} parameters are, as a rule, higher in absolute values for Np^{3+} than for Np^{4+} but not so much as could arise from average values of r^k, $k = 2, 4, 6$, for these ions. They are similar to those evaluated for U^{4+}. The last observation justifies our actual choice of CFPs used to simulate the electronic structure for the Np^{3+}:$ThCl_4$ system. The CFPs taken from the study on the U^{4+}:$ThCl_4$ system [19] were corrected using the ratios determined from the *ab initio* calculations (see table 3). The obtained energy levels are shown in figure 1 according to their polarization characteristic.

The actual task is to fit the energy levels provided by the model Hamiltonian to the observed electronic transitions by varying ten free parameters: three F^k, ζ, five B_{kq} and the most important correlation parameter α. The parameters β and γ have been fixed at the values taken from [10]. Various starting sets of parameters have been examined and various assignments of levels, since the selection rules for odd electron configurations are not very restrictive. The free ion parameters from the preceding Np^{4+} studies and the U^{4+} CFPs obtained for the same host or determined *ab initio* seemed to be a reasonable choice. Several solutions have been obtained with the r.m.s. error in the range 70–100 cm^{-1}, which was not very uncommon in the case of the neptunium ion [9, 16]. It was disturbing however that the observed relatively large splitting of the first excited term $^4I_{11/2}$ could not be reproduced satisfactorily. Therefore we started again with the levels confined to those belonging to the two lowest excited terms: $^4I_{11/2}$ and $^4F_{3/2}$. Then, step by step, the higher levels were included up to 27, the surest ones, described in the previous section. The remaining 14 transitions of limited confidence were added in the final steps.

The obtained model energy levels are compared with the observed transitions in table 4. They are also shown in figure 1. The corresponding parameters are given in table 5.

5. Discussion

The $5f^3$ electronic structure of the Np^{4+} ion in a $ThCl_4$ host is relatively dense and inherently complicated due to the extensive mixing between different multiplet manifolds. The presence of the Np^{3+} impurity in the measured samples makes an analysis of their optical spectra very difficult. Advanced spectroscopic techniques including polarized absorption and selective emission had to be complemented by the theoretical *ab initio* predictions and the information provided by still rather pure literature data. A comprehensive and compact

picture of localization and assignment of CF levels in the whole energy range was possible thanks to special treatment of the lowest infrared transitions, i.e. transitions observed in the areas which were free of Np^{3+} impurity. It should be emphasized that there was no other acceptable solution for this part of the spectrum but that presented here. Moreover, there was no exact solution for these several lowest lines. They could not be reproduced by any combination of 25 parameters of the model Hamiltonian. This points to the importance of the configuration mixing and the many-electron CF effects, which were not included in the present approach.

The final fit with the r.m.s. error of 36 cm^{-1} for 41 transitions seems to be satisfactory. All the observed main $\sigma\pi$ structures expected for Np^{4+} ($\Gamma_6 \rightarrow \Gamma_7$) have been considered as well as the manifest $\Gamma_6 \rightarrow \Gamma_6$ transitions σ except those observed in zone IV. The latter might be attributed, however to the Np^{3+} impurity.

Relatively large splitting of the first excited multiplet seen in the spectra led to crystal field parameters exceeding these expected from of the data known for the U^{4+} ion in the same host. It is hard to indicate on the ground of literature data any regularity concerning the behaviour of the CFPs along the f-electron series except discontinuity of their magnitudes in the middle of the series (see for instance [25]). Some heuristic arguments support believing that absolute values of the CFPs should decrease, going towards heavier f-electron elements [9]. The present *ab initio* calculations meet these expectations accurately but the phenomenological parameters shown in table 4, derived from the fittings, do not. In contrast, we see that the CF effect for Np^{4+} is stronger than for U^{4+}. In the case of zirconium silicate the difference in uranium and neptunium CF strength represented by the N_v parameter [26] (see footnote for table 3) is rather small. It is larger for thorium silicate and quite large in the case of thorium chloride.

Comparing the calculated *ab initio* CFPs with the phenomenological ones, table 3 and 5, one may note that the CF strength N_v is overestimated almost twofold for U^{4+} but is quite satisfactory for Np^{4+}. The corresponding CFPs are consistent only in the case of the most important parameter B_{44}. The largest discrepancy takes place for the parameters B_{20} and B_{40} for which the two co-ordination tetrahedra give contributions similar in absolute values but having opposite signs. We have already indicated that such a system was very sensitive to a small distortion of the metal environment. Replacement of the thorium ion with the doped one may cause a distortion and, in consequence, a discrepancy of the *ab initio* parameters with respect to the phenomenological ones. The distortion depends on the ionic radius so it may be different for the Np^{3+} and Np^{4+} ions.

Acknowledgment

One of us (ZG) would like to acknowledge financial support from the *Institut de Physique Nucleaire (Orsay)* during his two stays in *Laboratoire de Radiochimie* in 1996 and 1998. The other (JCK) wishes to express thanks to Norman Edelstein for partial support during a stay at Lawrence Berkeley Laboratory and George Shalimoff for his assistance in the measurements.

This work is dedicated to the memory of John Conway.

References

[1] Sharma K K and Artman J O 1969 *J. Chem. Phys.* **50** 1241
[2] Gruber J B and Menzel E R 1969 *J. Chem. Phys.* **50** 3772
[3] Menzel E R and Gruber J B 1971 *J. Chem. Phys.* **54** 3857

[4] Menzel E R, Gruber J B and Ryan J L 1972 *J. Chem. Phys.* **57** 4287
[5] Rajnak K, Banks R H, Gamp E and Edelstein N 1984 *J. Chem. Phys.* **80** 12
[6] Poirot I, Kot W A, Shalimoff G, Edelstein N, Abraham M M, Finch C B and Boatner L A 1988 *Phys. Rev.* B **11** 3255
[7] Lahalle M P 1986 *PhD Thesis* Universite Paris-Sud
[8] Lahalle M P, Krupa J C, Guillaumont R and Rizzoli C 1986 *J. Less-Common Met.* **122** 65
[9] Krupa J C 1987 *Inorg. Chim. Acta* **139** 223
[10] Krupa J C and Carnall W T 1993 *J. Chem. Phys.* **99** 8577
[11] Carnall W T, Liu G K, William C W and Reid M F 1991 *J. Chem. Phys.* **95** 7194
[12] Gajek Z, Mulak J, Krupa J C 1993 *J. Solid State Chem.* **107** 413
[13] Kern S, Lander G H, Soderholm L, Loong C K, Trouw F, West M, Hoisington D, Cort B and Welp U 1994 *J. Chem. Phys.* **101** 9338
[14] Burdick G W, Jayasankar C K, Richardson F S and Reid M F 1994 *Phys. Rev.* B **50** 16 309
[15] Faucher M D and Moune O K 1997 *Int. Conf. on f-Elements (Paris, 1997) Abstract Book* p 140
[16] Edelstein N 1987 *J. Less-Common Met.* **133** 39
[17] Kern S, Loong C K, Goodman G L, Cort B and Lander G H 1990 *J. Phys.: Condens. Matter* **2** 1933
[18] Krupa J C, Hubert S, Foyentin M, Gamp E and Edelstein N 1983 *J. Chem. Phys.* **78** 2175
[19] Khan Malek C, Krupa J C, Delamoye P and Genet M 1986 *J. Physique* **47** 1763
[20] Carnall W T, Crosswhite H, Crosswhite H M, Hessler J P, Edelstein N, Conway J G, Shalimoff G V and Sarup R 1980 *J. Chem. Phys.* **72** 5089
[21] Gajek Z, Mulak J and Faucher M 1987 *J. Phys. Chem. Solids* **48** 947
[22] Mucker K, Smith G S, Johnson Q and Elson R E 1969 *Acta Crystallogr.* B **25** 2362
[23] Hubert S, Delamoye P, Lefrant S, Lepostollec M and Hussonnois M 1981 *J. Solid State Chem.* **36** 36
[24] Erdos P and Kang J 1972 *Phys. Rev.* B **6** 3393
[25] Carnall W T, Goodman G L, Rajnak K and Rana R S 1989 *J. Chem. Phys.* **90** 3443
[26] Auzel F and Malta O 1983 *J. Physique* **44** 201